THE JOURNAL OF PHYSICAL CHEMISTRY C

ARTICLE

pubs.acs.org/JPCC

# Nanocrystalline Graphite Growth on Sapphire by Carbon Molecular Beam Epitaxy

S. K. Jerng,[†] D. S. Yu,[†] Y. S. Kim,[†] Junga Ryou,[†] Suklyun Hong,[*,†] C. Kim,[‡] S. Yoon,[‡] D. K. Efetov,[§] P. Kim,[§] and S. H. Chun[*,†]

[†]Department of Physics and Graphene Research Institute, Sejong University, Seoul 143-747, Korea

[‡]Department of Physics, Ewha Womans University, Seoul 151-747, Korea

[§]Department of Physics, Columbia University, New York, New York 10027, United States

**ABSTRACT:** We report the fabrication of nanocrystalline graphite films on sapphire substrates of various cutting directions by using solid carbon source molecular beam epitaxy. Raman spectra show a systematic change from amorphous carbon to nanocrystalline graphite with a cluster diameter of several nanometers, depending on the growth temperature. The symmetry of the substrate seems to have little effect on the film quality. Simulations suggest that the strong bonding between carbon and oxygen may lead to orientational disorders. Transport measurements show a Dirac-like peak and a carrier type change by the gate voltage.

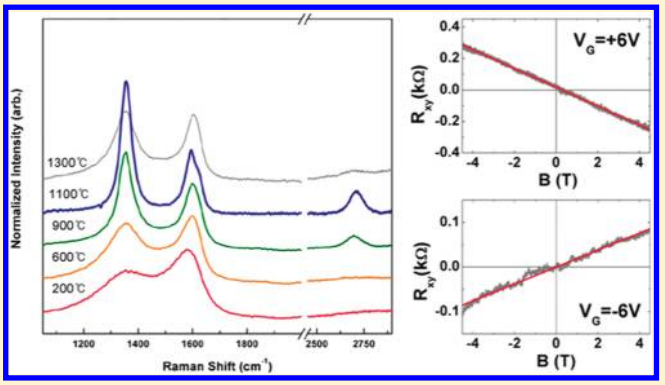


## 1. INTRODUCTION

Graphene has been attracting a great deal of attention because of its interesting physical behaviors and potential applications in a variety of fields.[1] In addition, the ease of graphene's preparation method, the mechanical exfoliation that requires only a roll of tape and graphite flakes,[2,3] helped the wide spread of graphene research. For applications, however, it is imperative to make high quality, large-scale graphenes reproducibly and cheaply. One graphene application is to provide a transparent and flexible electrode. In this case, the mass production of highly conductive graphene is important. The reduction of graphene oxide or chemical vapor deposition of graphene on metals has been studied to serve this purpose.[4−6] Another important application is to replace or complement current silicon technology, especially at the high-frequency regime. Recent reports of high-frequency transistors from graphene formed by thermal decomposition demonstrated the potential.[7,8]

Yet, if one can *grow* graphene directly on an insulating material and vice versa, it would accelerate integration of graphene with other materials such as semiconductors, ferromagnets, and ferroelectrics. New functional devices based on these hybrid multilayers are expected. Molecular beam epitaxy (MBE) is a good candidate to achieve this goal, as it has been widely used in the growth of complex multilayers with submonolayer accuracy. Furthermore, if successful, controlled doping of graphene would be easily accomplished. Several attempts were already tried with partial success: Hackley et al.[9] reported the growth of graphitic carbon on Si(111) and Moreau et al.[10] on SiC. However, the transport properties of these MBE-grown graphitic carbons or nanocrystalline graphites (NCGs) are unknown.

Here, we report our attempt to grow graphene on sapphire ($Al_2O_3$) substrates by MBE and the observation of a Dirac-like peak for the first time in MBE-grown NCGs. Sapphire has been chosen because of its hexagonal symmetry and the possibility of lattice-matched epitaxial growth [the in-plane lattice constant of (0001)-oriented sapphire, 4.75 Å, is about twice the graphene lattice constant, 2.45 Å]. The high melting point of sapphire (>2000 °C) is another benefit, since we expect that the graphene formation will be favored at high temperature. We varied the growth temperature over a wide range and studied the carbon bonding characteristics by Raman spectroscopy. Well-developed D, G, and 2D peaks from the optimized sample imply the formation of NCG,[11,12] and the ratio of D and G peaks suggests that its cluster diameter or in-plane correlation length is about 20 Å. Contrary to our expectation, we observed substrate orientation independence in growth mode. Ab initio simulations may explain such short correlation length and substrate orientation independence. Despite the disordered nature, an asymmetric Dirac-like peak was observed in the optimized sample and the change of carrier type from hole to electron was confirmed by Hall effect measurements.

**Received:** November 8, 2010
**Revised:** December 31, 2010
**Published:** March 02, 2011

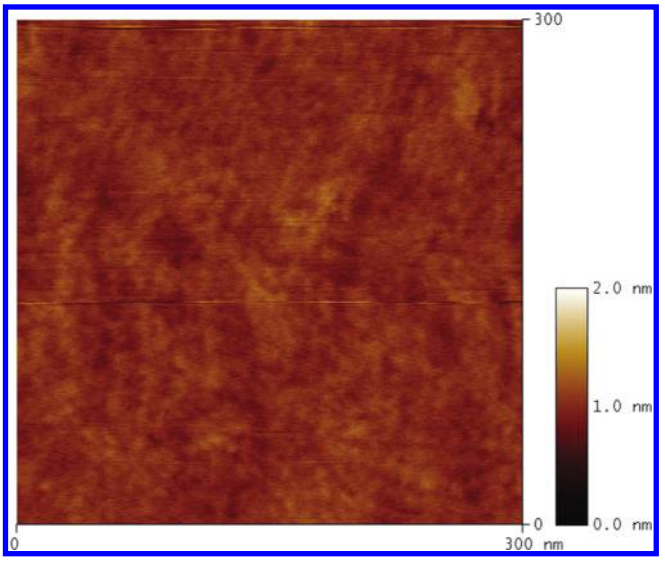


**Figure 1.** A 0.3 $\mu$m × 0.3 $\mu$m AFM image of a 3 nm-thick graphite film on sapphire grown at 600 °C. No noticeable features are seen. The mean roughness parameter, $R_a$, from 1 $\mu$m × 1 $\mu$m scan is 0.5 Å, similar to that of sapphire substrate before growth.

## 2. EXPERIMENTAL TECHNIQUES

For graphene growth we have built a dedicated ultrahigh vacuum (UHV) MBE system. High-purity pyrolytic graphite filament was heated to sublimate carbon (MBE-Komponenten GmbH). In order to achieve high substrate temperature beyond 1000 °C while allowing substrate rotation during growth, an electron beam from a tungsten filament was also used in heating the substrate holder made of Mo. We calibrated the thermocouple reading by measuring the desorption temperature of native oxide on Si wafer. Commercial sapphire substrates of various cutting planes (*C*, *R*, and *A* planes, 10 × 10 $mm^2$) were purchased and cleaned in acetone and isopropyl alcohol with ultrasonic. After introduction to the UHV system, each substrate was baked at 900 °C for 1 h to remove chemical residues. Then the substrate temperature was changed to the target temperature (200−1300 °C), where the growth started. The thickness of the sample, typically 3 nm, was determined by measuring the step height after lithography.

Room temperature Raman scattering measurements were performed by using a McPherson model 207 monochromator equipped with 600 grooves/mm gratings and a nitrogen-cooled charge-coupled device array detector. The excitation source was a 488 nm (2.54 eV) laser and the power used was 1.65 mW to avoid laser-induced surface heating and/or damage. The laser spot size was ∼1 $\mu$m in diameter focused by a 100× optical lens (numerical aperture = 0.95).

To investigate the initial growth of graphene on sapphire, we performed first-principles calculations within local density approximation (LDA) using the Vienna ab initio simulation package (VASP).[13,14] The ions are described by the projector augmented-wave potentials, and an energy cutoff of 282.6 eV is used. The carbon-adsorbed sapphire surface was modeled as a slab which consists of adsorbed carbon atoms and 18 sapphire layers (12 aluminum and 6 oxygen atomic layers) with the vacuum region being about 10−15 Å. Geometries were optimized until the Hellmann−Feynman forces were smaller than 0.03 eV/ Å.

To measure the transport properties, samples were patterned to Hall bars by electron beam lithography. The top gate was formed by successive deposition of HSQ, $HfO_2$, and Cr/Au on the sample. Resistance was measured by using a standard ac method. Details of the fabrication process can be found elsewhere.[15]

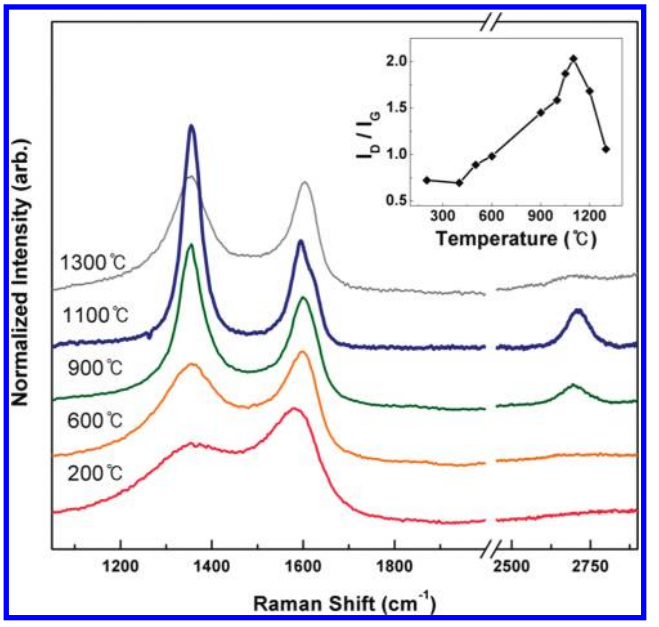


**Figure 2.** Raman spectra of NCG films grown at different temperatures. The characteristic peaks of NCG (D peak near 1350 $cm^{-1}$ and G peak near 1600 $cm^{-1}$) are seen for all the samples. 2D peak near 2700 $cm^{-1}$ is also observed for the samples grown at high temperatures. The inset is the dependence of the D peak to G peak height ratio on the growth temperature.

## 3. RESULTS AND DISCUSSION

The surfaces of as-deposited samples on *C* plane sapphires were flat with no sign of island growth. Even the atomic force microscope images did not show any noticeable feature (Figure 1). Indeed, the roughness was the same before and after the growth (0.5 Å for 1 $\mu$m × 1 $\mu$m scan), irrespective of the growth temperature ($T_G$).

For all the samples, the characteristic peaks of carbon $sp^2$ bonding were observed in the Raman spectra as shown in Figure 2: D peak near 1350 $cm^{-1}$ and G peak near 1600 $cm^{-1}$. For samples grown at $T_G \geq 900$ °C, the 2D peak was observed at near 2700 $cm^{-1}$.[11,12] The sharpness and the relative strength of D and G peaks ($I_D/I_G$) depend strongly on $T_G$. The inset of Figure 2 shows that $I_D/I_G$ increases and reaches to 2.1 as $T_G$ increases from 200 to 1100 °C and decreases sharply on further increase of $T_G$. According to the three-stage model of Ferrari and Robertson, $I_D/I_G$ can be used to estimate $sp^2$-bonded cluster size or in-plane correlation length, $L_a$.[11] Theoretically this ratio increases from 0 to 2.4 as the amorphous carbon becomes NCG (stage 2) and then decreases again to 0 as the cluster size of graphite becomes infinite (stage 1). A recent study on electron-beam-irradiated graphene confirmed this model experimentally.[16]

It is concluded that the samples belong to stage 2 from the sharpness of the D and G peaks. Well-developed Raman peaks in the optimized sample imply the formation of NCG.[11,12] The peaks become sharp as $T_G$ increases, and then broaden again for samples grown at $T_G > 1100$ °C. The simultaneous decrease of D and 2D peaks when $T_G > 1100$ °C support this conclusion, since we expect an increase of 2D peak intensity in stage 1 (Figure 2).

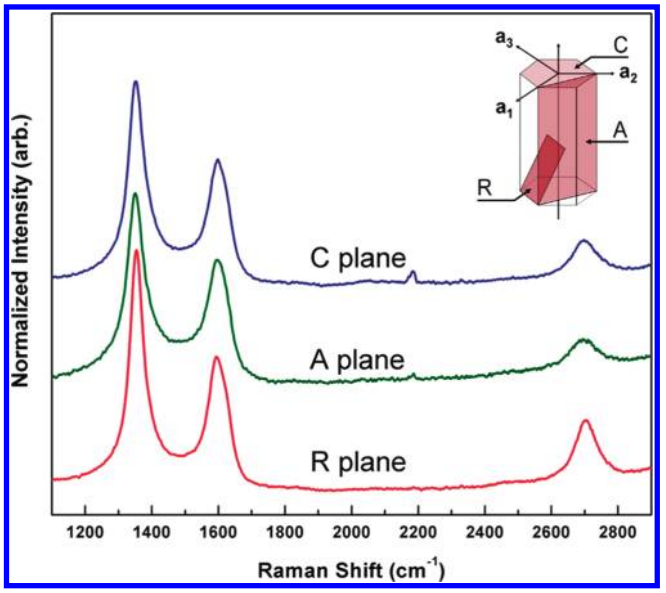


**Figure 3.** Raman spectra of the optimized NCGs grown on sapphire substrates of different planes (*C*, *R*, and *A* planes). The inset shows the cutting directions. Overall, the Raman spectra are similar for all the planes investigated, implying that the symmetry and the lattice constant of the substrate do not affect the sample quality in this experiment.

In stage 2, $I_D/I_G$ is proportional to $L_a^2$, and for samples grown at $T_G$ = 1100 °C, $L_a$ is estimated to be about 20 Å or larger.[11,17,18] These imply that the film mainly consists of graphitic carbons. The position of the G peak is another piece of evidence that the optimized sample is NCG.[11,19]

In order to understand the effect of substrate symmetry while keeping chemical interaction intact, we grew several samples on sapphire of different cutting planes. We chose orientations of (1102) (*R* plane) and (11$\bar{2}$0) (*A* plane), which were commercially available and possessed similar surface roughness to (0001) (*C* plane) oriented substrates. As shown in the inset of Figure 3, both have rectangular symmetry in contrast to *C* plane sapphire and graphene having hexagonal symmetries. We also varied $T_G$ for each orientation, and found that the optimum growth temperature was unchanged (1100 °C). Contrary to our belief, we found the samples grown on sapphire with different symmetries and lattice constants (*R* and *A* planes) show similar Raman spectra. Figure 3 shows that the degree of disorder and the cluster size are similar for all the orientations tested, except a slight change in the 2D peak height. Such independence of sample quality on the substrate orientation implies that chemical interaction between the substrate and carbon is more important than lattice matching.

To understand the initial stage of graphene growth, we investigate the adsorption of carbon atoms or carbon cluster on sapphire.[13,14] For the adsorption of a single carbon atom, the binding of carbon to oxygen atom on sapphire is more favorable in energy by 2.78 eV than that to aluminum atom. Two carbon atoms formed a dimer on sapphire bound to oxygen and aluminum atoms, respectively, while three carbon atoms form a somewhat linear structure attached to an oxygen surface atom. By increasing the number of adsorbed carbon atoms up to 20 on the sapphire surface, we found the following adsorption behaviors. In the optimized structures with the lowest energy, (i) the carbon atoms form a distorted honeycomb-like or graphene-like structure, and (ii) one carbon atom of the entire carbon structure

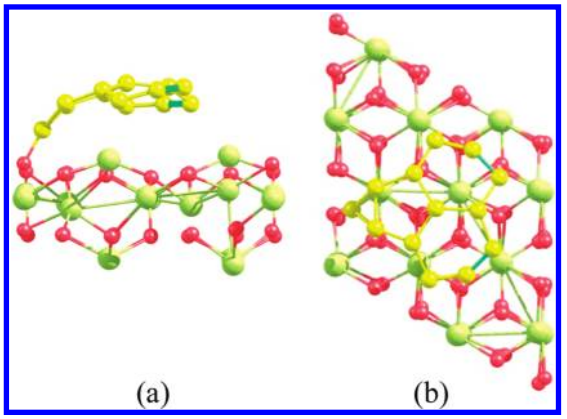


**Figure 4.** Optimized configuration of 13 carbon atoms adsorbed on *C* plane sapphire. One carbon atom of a distorted graphene-like structure (yellow) binds to an oxygen atom (red), rather than to aluminum (green): (a) side view and (b) top view.

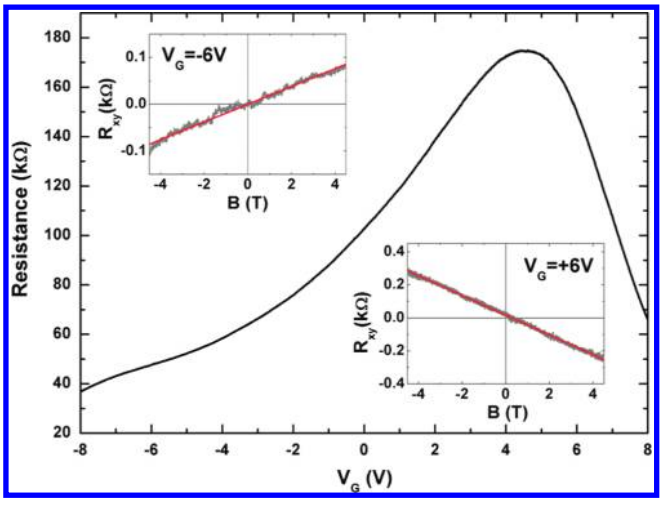


**Figure 5.** Dependence of room temperature resistance on the gate voltage, showing an asymmetric Dirac-like peak. The insets are Hall effect measurements under gate voltage of −6 V (left inset) and +6 V (right inset) showing the carrier type change from hole (positive slope) to electron (negative slope). The solid lines in the insets are linear fitting for carrier density calculation.

binds to an oxygen atom of sapphire due to strong binding of carbon with oxygen atoms (see Figure 4). Therefore, unless it is initially covered by a perfect graphene sheet, the sapphire surface binds with carbon structures by strong interaction between carbon and oxygen atoms. On the basis of our theoretical results, we can speculate the following. In the MBE experiment, carbon cluster fragments consisting of at least several carbon atoms adsorb on the sapphire surface and accumulate to form a honeycomb-like structure due to very strong binding between carbon atoms. While forming such a carbon structure, carbon atoms start to interact with oxygen atoms, binding between (at least) one carbon atom of the carbon structure and an oxygen atom. Such a binding is expected to occur somewhat randomly, depending on the formation rate of the graphene-like structure and the diffusion rate of carbon atoms.[20] Accordingly, strong binding between carbon and oxygen may lead to segregation of graphene-like structures in a limited area rather than a perfect graphene formation. Thus, ab initio calculations may (partly) explain the short correlation length and substrate orientation


dx.doi.org/10.1021/jp110650d |*J. Phys. Chem. C* 2011, 115, 4491–4494

independence in growth mode. Combined with this explanation, the observed flatness of films suggests that the main disorder must be orientational.

Now we turn to the transport properties. All the samples except ones grown at 400 °C are conducting at room temperature. Two-probe conductance increases as $T_G$ increases and then decreases as $T_G$ goes beyond 1100 °C, similar to the behavior of $I_D/I_G$ with $T_G$. This is in accord with our conclusion that the samples belong to stage 2: at this stage, $I_D/I_G$ increases on increasing $L_a$; therefore, the conductivity increases, too.[11] Samples of relatively high conductance were processed into Hall bars with metal top gates. Even for samples of room temperature resistance larger than 100 kΩ, we were able to observe Dirac-like peaks. Figure 5 shows the result of a sample grown at $T_G$ = 1100 °C. The Dirac-like peak is asymmetric and the center is shifted by more than 5 V. The asymmetry is observed for all the samples processed, but the shift is sample-dependent. Reliable Hall effect measurements, however, were possible only for the sample grown at $T_G$ = 1100 °C. The insets of Figure 5 show the change of carrier type from hole to electron by the gate voltage ($V_G$), confirmed by Hall effect measurements. The carrier density is about $\sim 10^{13}$ cm$^{-2}$ and the mobility is on the order of $\sim$1 cm$^2$/(V s) at $V_G = \pm 6$ V. Although the mobility is very small at present, improvements are expected as the growing methods are advanced.

## 4. CONCLUSIONS

To summarize, we have succeeded in growing NCG on sapphire substrates of different orientations by solid source carbon MBE. Raman spectra depend strongly on the growth temperature of films and show well-developed D, G, and 2D peaks for optimized samples, which indicates the formation of NCG. From the ratio of D and G peak intensities, the cluster diameter or in-plane correlation length of NCG is presumed to be about 20 Å. The experimentally observed independence of cluster size on the substrate direction is partly explained by ab initio calculations. In addition, we observed a Dirac-like peak and a carrier type change by the gate voltage for the first time in MBE-grown NCGs. Heterostructures of NCGs and other materials, all fabricated by MBE, may find interesting applications in the future.

## AUTHOR INFORMATION

### Corresponding Author

*Fax: +82 2 3408 4316. E-mail: schun@sejong.ac.kr (S.H.C.), hong@sejong.ac.kr (S.H.).

## ACKNOWLEDGMENT

This research was supported by the Midcareer Researcher Program (2009-0052981, 2010-0000053), the Converging Research Center Program (2010K001069), Priority Research Centers Program (2010-0020207), and the Basic Science Research Programs (KRF-2008-313-C00217, KRF-313-2007-2-C00231, 2010-0024426) through the National Research Foundation of Korea (NRF) funded by the Ministry of Education, Science and Technology (MEST). Calculations were performed by using the supercomputing resources of KISTI.

## REFERENCES

(1) Geim, A. K.; Novoselov, K. S. *Nat. Mater.* **2007**, *6* (3), 183–191.
(2) Novoselov, K. S.; Geim, A. K.; Morozov, S. V.; Jiang, D.; Zhang, Y.; Dubonos, S. V.; Grigorieva, I. V.; Firsov, A. A. *Science* **2004**, *306*, 666–669.
(3) Novoselov, K. S.; Jiang, D.; Schedin, F.; Booth, T. J.; Khotkevich, V. V.; Morozov, S. V.; Geim, A. K. *Proc. Natl. Acad. Sci. U. S. A.* **2005**, *102*, 10451–10453.
(4) Dikin, D. A.; Stankovich, S.; Zimney, E. J.; Piner, R. D.; Dommett, G. H. B.; Evmenenko, G.; Nguyen, S. T.; Ruoff, R. S. *Nature* **2007**, *448*, 457–460.
(5) Kim, K. S.; Zhao, Y.; Jang, H.; Lee, S. Y.; Kim, J. M.; Kim, K. S.; Ahn, J.-H.; Kim, P.; Choi, J.-Y.; Hong, B. H. *Nature* **2009**, *457*, 706–710.
(6) Li, X.; Cai, W.; An, J.; Kim, S.; Nah, J.; Yang, D.; Piner, R.; Velamakanni, A.; Jung, I.; Tutuc, E.; Banerjee, S. K.; Colombo, L.; Ruoff, R. S. *Science* **2009**, *324*, 1312–1314.
(7) Moon, J. S.; Curtis, D.; Hu, M.; Wong, D.; McGuire, C.; Campbell, P. M.; Jernigan, G.; Tedesco, J. L.; VanMil, B.; Myers-Ward, R.; Eddy, C.; Gaskill, D. K. *SIEEE Electron Device Lett.* **2009**, *30*, 650–652.
(8) Lin, Y.-M.; Dimitrakopoulos, C.; Jenkins, K. A.; Farmer, D. B.; Chiu, H.-Y.; Grill, A.; Avouris, Ph. *Science* **2010**, *327*, 662.
(9) Hackley, J.; Ali, D.; DiPasquale, J.; Demaree, J. D.; Richardson, C. J. K. *Appl. Phys. Lett.* **2009**, *95* (13), 133114.
(10) Moreau, E.; Ferrer, F. J.; Vignaud, D.; Godey, S.; Wallart, X. *Phys. Status Solidi A* **2010**, *207* (2), 300–303.
(11) Ferrari, A. C.; Robertson, J. *Phys. Rev. B* **2000**, *61* (20), 14095–14107.
(12) Ni, Z. H.; Chen, W.; Fan, X. F.; Kuo, J. L.; Yu, T.; Wee, A. T. S.; Shen, Z. X. *Phys. Rev. B* **2008**, *77* (11), 115416.
(13) Kresse, G.; Furthmüller, J. *Phys. Rev. B* **1996**, *54* (16), 11169–11186.
(14) Kresse, G.; Furthmüller, J. *Comput. Mater. Sci.* **1996**, *6* (1), 15–50.
(15) Han, M. Y.; Ozyilmaz, B.; Zhang, Y.; Kim, P. *Phys. Rev. Lett.* **2007**, *98* (20), 206805.
(16) Teweldebrhan, D.; Balandin, A. A. *Appl. Phys. Lett.* **2009**, *94* (1), 013101.
(17) Nemanich, R. J.; Solin, S. A. *Phys. Rev. B* **1979**, *20* (2), 392–401.
(18) Lespade, P.; Al-Jishi, R.; Dresselhaus, M. S. *Carbon* **1982**, *20* (5), 427–431.
(19) Calizo, I.; Bao, W.; Miao, F.; Lau, C. N.; Balandin, A. A. *Appl. Phys. Lett.* **2007**, *91* (20), 201904.
(20) Shin, Y.-H.; Hong, S. *Appl. Phys. Lett.* **2008**, *92* (4), 043103.